

Measurement of the Casimir force between Germanium plates using a torsion balance

W. J. Kim,¹ A.O. Sushkov,¹ D. A. R. Dalvit,² and S. K. Lamoreaux¹

¹*Yale University, Department of Physics, P.O. Box 208120, New Haven, CT 06520, USA*

²*Theoretical Division, MS B213, Los Alamos National Laboratory, Los Alamos, NM 87545, USA*

(Dated: November 15, 2021)

We report the measurement of the Casimir force between Ge plates in a sphere-plane configuration using a torsion balance. We observe that the effective contact potential between the plates varies with their separation distance, resulting in a systematic force. In addition, an unexpected $1/d$ force is also found in our data that persists even when the electrostatic force between the plates is experimentally minimized by applying a compensating potential. After applying corrections due to these systematic forces, likely of electrostatic origin, our result can be described by the bare permittivity of Ge without conduction, the Drude and the diffusion models for electrical and optical properties of Ge, but not by the plasma model.

PACS numbers: 12.20.Fv, 11.10.Wx, 73.40.Cg, 04.80. Cc

The Casimir force has been a subject of great interest, both theoretically and experimentally, because it is a macroscopic manifestation of the quantum vacuum effects [1, 2, 3]. The recognition that, by use of modern experimental techniques including automated data acquisition [4], precision measurements of this force are possible has stimulated experimental activity [5] over the last decade. At present, interest in precision measurements has been sparked by the controversies surrounding various models of the electrical permittivity of the plates and the field interactions, together with the finite temperature correction [6, 7], required for calculations using the Lifshitz formalism [8]. For example, only in the plasma model does the transverse-electric zero-Matsubara-frequency mode contribute to the force, making it about 20% larger at distances around $1 \mu\text{m}$ at $T=300 \text{ K}$ for most metals. The lack of contribution of this mode in all but the plasma model reflects the fact that a static magnetic field does not interact with a non-magnetic conductor, while several experiments, perhaps most notably [4], suggest its inclusion. Experimental studies present great challenges because precision measurements require careful assessment of possible spurious systematic effects. A recent study [9] as well as early investigations of a short-range force [10, 11] report the possible systematic effects due to residual electrostatic forces. The optical response of a particular sample under study must also be carefully considered [12], as the accuracy of data on the optical properties of materials typically limits calculational accuracy to no better than 5%.

In this Letter, we present results of force measurements between crystalline Ge plates [13] in a sphere-plane geometry. Our apparatus, shown schematically in Fig. 1, is based on the design presented in [14] and improves on the apparatus described in [4, 16]. On one side of the torsion pendulum a flat Ge plate is mounted, and approached by a Ge plate with a spherical surface, with radius of curvature $R = (15.10 \pm 0.05) \text{ cm}$, that is mounted on a Thor-

labs T25 XYZ motion stage (40 nm resolution). When a force exists between these plates, the torsion body rotates and thereby generates an imbalance in capacitance on the the other side of the pendulum, which carries a flat plate, situated in between two fixed “compensator plates”, that are attached to the support frame. An AC voltage is applied to the compensator plates, and the capacitance imbalance creates an AC voltage that is amplified and sent to a phase sensitive detector (PSD), providing an error signal to a proportional-integral-differential (PID) feedback circuit. A small correction voltage (S_{PID}) is applied to the compensator plates keeping the system in equilibrium. The correction voltage is added to a large constant voltage $V_0 (\approx 9 \text{ V})$ to linearize the restoring force, $F \propto (S_{\text{PID}} + V_0)^2 \approx V_0^2 + 2V_0 S_{\text{PID}}$. This correction voltage provides a measure of the force between the Casimir plates and is recorded during the measurement.

The measured signal S_{PID} has contributions from several sources:

$$S_{\text{PID}}(d, V_a) = S_{\text{DC}}(d \rightarrow \infty) + S_c(d) + S_p(d, V_a), \quad (1)$$

where S_{DC} is the force-free component of the signal at a large distance, S_c is the signal subject to distance-dependent forces, such as Casimir-Lifshitz force, and S_p is the electric force in response to an externally applied voltage V_a . Assuming a value of contact potential V_c that does not depend on d , the electrostatic contribution S_p due to V_a in the sphere-plane geometry can be written as, when $d \ll R$, by use of the Proximity Force Approximation (PFA)

$$S_p(d, V_a) = \frac{\pi\epsilon_0 R (V_a - V_c)^2}{\beta d}, \quad (2)$$

where β is a calibration factor that converts S_{PID} in units of voltage to the actual units of force. Note that the electrostatic force is minimized ($S_p = 0$), when $V_a = V_c$, and the electric force minimizing potential V_m is the contact potential between the plates. This is true only

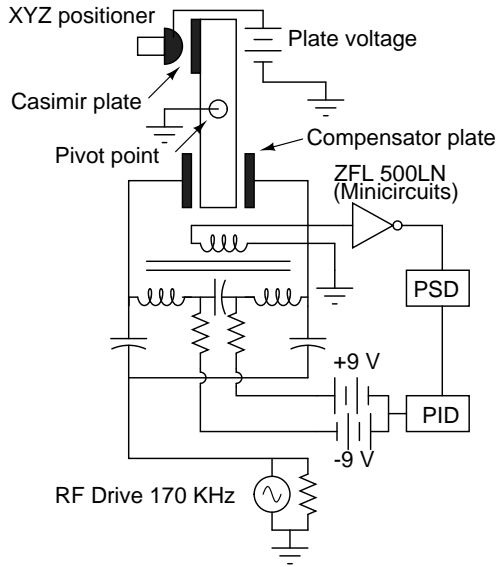


FIG. 1: Experimental setup of torsion balance from top-view. A pendulum body of length 15 cm hangs from a tungsten wire connected to a motorized rotation stage via the pivot point that is mounted on a support frame. The wire diameter is 25 μm , with length 2.5 cm, shorter than the previous experiment (66 cm) [4] in order to minimize effects of tilt of the apparatus. At the bottom of the pendulum body (not shown in the figure) is an NdFeB magnet to damp the swinging modes of the pendulum at a natural frequency of 3 Hz. The mechanical assembly is covered by a glass bell jar (vacuum 5×10^{-7} torr) and is supported on a vibration isolation slab that has its foundation separate from the laboratory building.

if V_c does not depend on distance. Next, a range plate voltages V_a are applied, and at a given separation the response S_{PID} is fitted to a parabola

$$S_{\text{PID}}(V_a) = S_0 + k(V_a - V_m)^2. \quad (3)$$

The first two terms in Eq. (1) are absorbed by S_0 and represent the minimized signal when $V_a = V_m$. Repeating the parabola measurements shown in Fig. 2a, sequentially moving from the farthest to closest plate separations, enables us to inspect the d dependence of the fitting parameters $k(d)$, $V_m(d)$, and $S_0(d)$. The procedure outlined here was first implemented as a calibration routine in [17] and more recently in [9] in an effort to detect a distance dependence of V_m .

As the gap between the plates is reduced, the parabola curvature k rapidly increases as shown in Fig. 2b. These curvature values are fitted to $k(d) = \alpha/d$, the expected dependence for the plane-sphere geometry, where the absolute distance $d \equiv d_0 - d_r$ is defined in terms of the asymptotic limit d_0 and the relative distance d_r recorded during a parabola measurement. The conversion factor β is then obtained through $\alpha \equiv \pi\epsilon_0 R/\beta$. Obviously, α can be also used to determine the absolute distance through $d = \alpha/k$, implying a significant correlation of α with d_0 . Consistency between these two sets of distance determi-

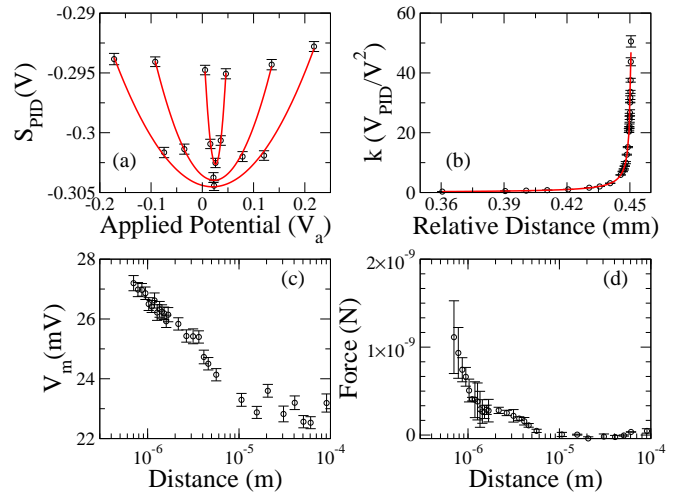


FIG. 2: Description of procedure for force analysis. (a) A single parabola measurement at a given distance is acquired by sweeping a range of voltage differentials applied to the plates. The procedure is repeated at incremental distances from 150 μm down to 500 nm, completing a single experimental run. The parabolic curves shown here represent only three distances, 100 μm , 20 μm , and 1 μm for clarity. (b) Curvature coefficients of the parabola k versus relative distances were fitted to the $1/d$ electric force to provide the voltage-to-force conversion factor β as well as the absolute distance obtained from an asymptotic limit. (c) The force-minimizing potential changes with distances, varying approximately linearly with $\log d$. (d) The residual force at the minimizing potential is plotted against distances, after subtracting the DC offset S_{DC} and multiplying it by β . The maximum force gradient for feedback system stability is 5 $\text{nN}/\mu\text{m}$, limiting the minimum distance to 500 nm.

nation reflects validity of the use of the $1/d$ power law as implied by a value of χ_0^2 close to unity for our data set (see below). Fig. 2c shows the electric potentials at minima of the parabola curvatures plotted with respect to d , indicating the distance-dependent minimizing potential $V_m(d)$, a behavior that has been observed in other experiments [9, 18]. This variation leads to a force beyond Eq. (2). The electrostatic force is the gradient of the electrostatic energy $E_e(d) = C(V_a - V_c(d))^2/2$, where $C = C(d)$ is the capacitance between the plates, and we define an attractive force between the plates as positive. Writing $C' = \partial C/\partial d$, the condition for the force minimum with respect to V_a satisfies [15]

$$C'(V_m(d) - V_c(d)) = C \frac{\partial V_c(d)}{\partial d}. \quad (4)$$

Clearly, the potential that sets a parabola minimum V_m acquired during a measurement is no longer equal to V_c , and one must solve the first-order differential equation in Eq. (4) to find the true contact potential that appears in the energy equation. Moreover, the variation in contact potential gives rise to a systematic residual force that contributes to the minimized signal S_0 , which

is determined, using Eq. (4) to obtain V_c , by

$$\beta S_r = F_r(d) = \frac{C^2}{2C'} \left(\frac{\partial V_c}{\partial d} \right)^2 = \frac{C'}{2} (V_m(d) - V_c(d))^2, \quad (5)$$

which is a *repulsive* force because $C' < 0$. The force appearing in Eq. (5) should be understood as an attractive force that has not been fully compensated due to the distance-dependent contact potential, rather than the actual physical force of repulsion between the plates.

To see the trend in $V_m(d)$ more clearly and to determine the Casimir force with higher statistical accuracy, we have repeated, 193 times, the experimental sequence described in Fig. 2, yielding a total of 5900 data points. Each group of five data points taken at a given fixed distance with varying applied potential are used to determine the three parabola parameters discussed above, in addition to the force and distance. The mean value of the calibration factor after analyzing all data is $\beta = (1.281 \pm 0.003) \times 10^{-7}$ N/V with an average χ_0^2 of 1.2. The uncertainty on the power $1/d^n$ when left as a free parameter is $n = 0.9979 \pm 0.002$ with $\chi_0^2 = 1.01$. Both the asymptotic limit d_0 shown in Fig 2b and the DC offset of the PID signals S_{DC} drifts slightly during a run. The uncertainty in position is about 50 nm, roughly 10 % of the typical closest gap separation. The DC offset drift has been corrected by monitoring S_{PID} before and after each consecutive runs and applying a linear correction.

The capacitance between the plates, as a function of d , was measured by use of a relaxation oscillator for distances above 10 μm . A PFA calculation of the capacitance, as used in Eq. (4) and Eq. (5), agrees well with this direct measurement. The use of $C' = 2\pi\epsilon_0 R/d$ in the force calibration is verified; the agreement of the measured k values to the $1/d$ and consistency of all relevant parameters, such as β and d_0 from different runs, indicates a great degree of reliability and reproducibility of the force measurements as well as the distance characterization.

The residual electrostatic correction F_r is determined from Eq. (5) using V_c obtained by solving Eq. (4). A functional form of $V_m(d)$ is obtained by fitting to a cubic polynomial of $\log d$ at short distance ($< 30 \mu\text{m}$), and by a spline interpolation of $\log d$ at larger distances (see Fig. 3). The residual force is subtracted from the raw data $\beta(S_0 - S_{DC})$, which is the first correction applied to the data and has no adjustable parameters. In addition, a $1/d$ force, of unknown origin, is clearly evident in our data as shown on top of Fig. 4. Using data for $d > 1.5 \mu\text{m}$, for which no significant Casimir force contribution is expected, the force is determined by least squares fitting to $a_0 + a_1/d$ with $a_0 = (-9 \pm 7) \times 10^{-12}$ N and $a_1 = (4.3 \pm 0.3) \times 10^{-10}$ N μm . The exponent in $1/d^n$ was independently determined to be $n = 0.98 \pm 0.07$, confirming the presence of such a systematic long-range force in the distance regime $d > 1.5 \mu\text{m}$. This is the

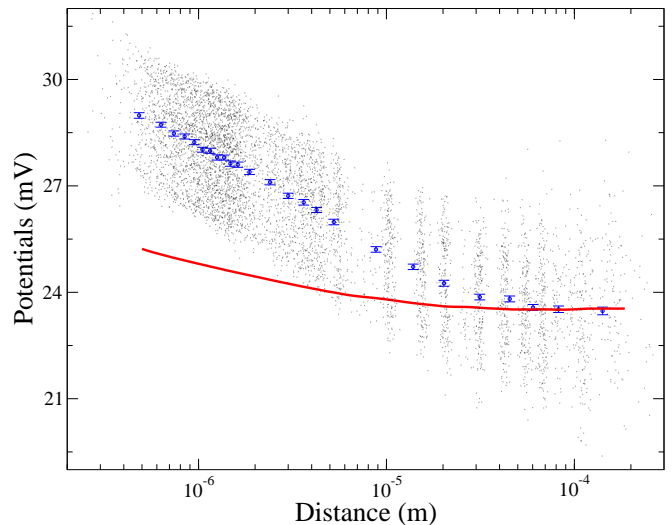


FIG. 3: The value of the force minimizing potential as a function of plate separation. Our data set reveals a slow rise of the minimizing potential as the plates approach each other, of order of 8 mV over 100 μm . The average values represented by the dotted line (blue) are based on 5900 points of V_m from the 193 experimental runs and are used in the numerical solution of the contact potential differential equation in Eq. (4), to obtain V_c indicated by the solid line (red).

only adjustable fitted correction in our analysis. With these two principal corrections, both of apparent electrostatic origin, the final corrected data agree well with all Ge plate models except the plasma model (see caption of Fig. 4).

There are several systematic effects we consider for the observation of the long-range $1/d$ force in our data. By direct measurement, we find no spurious AC voltage between the plates, which would need to be of order 6 mV to create the observed effect. Other possibilities include, but are not limited to, the attraction between charges in surface states on one plate and their images on the other plate, and the existence of large scale potential patches on the surfaces, as previously considered an origin of long-range surface force in a van der Waals force measurement [10]. These effects are not mutually exclusive. In order to test the large patch potential hypothesis, we have measured the effective contact potential as a function of position across the plates, and indeed there is a change in potential near the edge of the curved plate. This simple model which is valid when the patch dimensions are much larger than the largest separations between the plates, also shows that a slow radial variation of the surface potential can produce the observed $V_m(d)$, while large scale random fluctuations with zero net average will produce a $1/d$ potential. Surface roughness based on the quoted 60/40 scratch dig surface finish, independently verified by SEM measurements, leads to less than 1% correction. The plates were cleaned several times over the course of

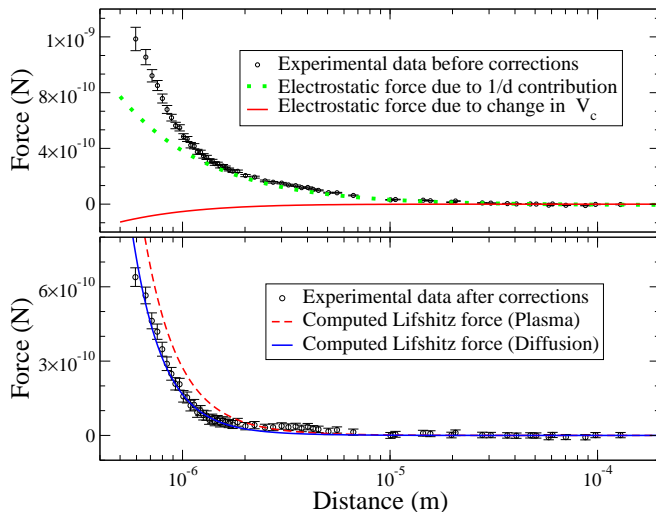


FIG. 4: (top) Two major corrections are applied to our averaged raw data. The correction due to the variation in V_c (violet curve), as described by Eq. (5), is subtracted from the raw data followed by a determination and subtraction of the $1/d$ correction (dotted green). (bottom) The final corrected data are shown along with two theoretical models, the plasma model and the diffusion model [20]. For the bare permittivity (ignoring conduction), the diffusion and Drude models, which lie within 5% to 10% of each other over the 0.5 to 1.5 μm distance range, the agreement with theory can be determined by χ_0^2 , which are 0.30, 0.55, 1.06, respectively, while the plasma model gives $\chi_0^2 = 11.7$ (prob. $< 0.001\%$). The Ge optical and electrical parameters listed in [20] were used for the theoretical calculations. The errors in the lower plot were increased to account for the finite precision of the $1/d$ fit and to account for the non-gaussian character of the noise.

the measurements, and once etched in dilute hydrofluoric acid which is known to provide a hydrogen passivated surface [19]. No discernible change in the character of the force or minimizing potential was observed. Finally, we had expected that the capacitance between the plates would be modified at close distances due to the finite Debye length penetration of the electric field into Ge, resulting is a saturation of the capacitance at very short distances and a correction to the distance determination. This effect should have been observed as a deviation of the parabola curvature coefficients from a $1/d$ law, but the effect was apparently canceled by redistribution of surface charges, providing further evidence for their expected existence.

In conclusion, we have performed a measurement of the Casimir force between crystalline Ge plates. The contact potential between the plates was found to be distance-dependent and this variation causes a repulsive residual electrostatic force that can be calculated. In addition, a $1/d$ force is observed in the data whose specific origin is unproven. Our result invalidates the plasma model as applied to Ge, but is not of sufficient accuracy to discriminate between the simple dielectric permittivity of

Ge, the Drude model, or the diffusion model presented in [20]. Given the number of corrections that needed to be applied, our conclusions must be regarded as provisional. We further point out that, in our early stages of our work with Ge plates [16], we assumed that the contact potential was constant and equal to its long range value, and we held the applied potential at a fixed value in our measurements. Fitting to and subtracting only a $1/d$ potential leaves the residual *attractive* potential which has sufficient magnitude to make the data agree better with the plasma model [16]; this was possibly a systematic in [4]. We hope to extend these measurements to metallic films in the near future. We acknowledge support by Yale University for construction of the experimental apparatus and data acquisition, and by Los Alamos LDRD program for theoretical calculations. We acknowledge fruitful discussions with Roberto Onofrio and Sven de Man.

-
- [1] H. G. B. Casimir, Proc. K. Ned. Akad. Wet. **51**, 793 (1948).
 - [2] P.W. Milonni, *The Quantum Vacuum* (Academic Press, San Diego, 1994).
 - [3] M. Bordag, U. Mohideen, and V. M. Mostepanenko, Phys. Rep. **353**, 1 (2001).
 - [4] S. K. Lamoreaux, Phys. Rev. Lett. **78**, 5 (1997).
 - [5] U. Mohideen and A. Roy, Phys. Rev. Lett. **81**, 4549 (1998); H. B. Chan *et al.*, Science **291**, 1941 (2001); G. Bressi *et al.*, Phys. Rev. Lett. **88**, 041804 (2002); R. S. Decca *et al.*, *ibid.* **91**, 050402 (2003).
 - [6] M. Bostrom and Bo. E. Sernelius, Phys. Rev. Lett. **84**, 4757 (2000).
 - [7] I. Brevik *et al.*, New J. Phys. **8** 236 (2006).
 - [8] E. M. Lifshitz, Sov. Phys. JETP **2**, 73 (1956).
 - [9] W. J. Kim *et al.*, Phys. Rev. A **78**, 020101(R) (2008); W. J. Kim *et al.*, e-print arXiv:0812.0328.
 - [10] N. A. Burnham, R. J. Colton, and H. M. Pollock, Phys. Rev. Lett. **69**, 144 (1992).
 - [11] B. C. Stipe *et al.*, Phys. Rev. Lett. **87**, 096801 (2001).
 - [12] V. B. Svetovoy *et al.*, Phys. Rev. B **77**, 035439 (2008).
 - [13] We chose Ge for our measurements because it is among the purest materials available, optical components made of intrinsic crystalline Ge are readily available, and its properties are well-tabulated (ISP optics GE-PX-25-50).
 - [14] S. K. Lamoreaux and W. T. Buttler, Phys. Rev. E **71**, 036109 (2005).
 - [15] S. K. Lamoreaux e-print arXiv: 0808:0885.
 - [16] Fan Xiao, Ph.D. Dissertation, Yale University, New Haven (2008).
 - [17] D. Iannuzzi *et al.*, Proc. Nat. Ac. Sci. USA **101** 4019 (2004).
 - [18] S. de Man, K. Haek, and D. Iannuzzi, e-print arXiv:0809.3858.
 - [19] S. Sun *et al.*, Appl. Phys. Lett **88** 021903 (2006).
 - [20] D. A. R. Dalvit and S. K. Lamoreaux, Phys. Rev. Lett. **101**, 163203 (2008).